Microbiological Research 293 (2025) 128053

Contents lists available at ScienceDirect

Microbiological Research

journal homepage: www.elsevier.com/locate/micres

Akkermansia muciniphila inhibits jejunal lipid absorption and regulates jejunal core bacteria

Qiming Ma [b,c], Xincheng Zhou [b,c], Weikang Su [b,c], Qingyu Wang [b,c], Guoxing Yu [b,c], Weihua Tao [b,d], Zhiyong Dong [b,c], Cunchuan Wang [b,c], Chi-Ming Wong [e], Tiemin Liu [a,f,*], Shiqi Jia [a,b,c,*,1]

[a] Institutes of Biomedical Sciences, College of Life Sciences, Inner Mongolia University, Hohhot, China
[b] The First Affiliated Hospital of Jinan University, Guangzhou, China
[c] The Guangdong-Hong Kong-Macao Joint University Laboratory of Metabolic and Molecular Medicine, Jinan University, Guangzhou, China
[d] Biobank of the First Affiliated Hospital of Jinan University, Guangzhou, China
[e] Department of Health Technology and Informatics, Hong Kong Polytechnic University, Hong Kong
[f] School of Life Sciences, Fudan University, Shanghai, China

ARTICLE INFO

Key words:
Akkermansia muciniphila (Akk)
Jejunal epithelial cells
AMP-activated protein kinase (AMPK)
Lipid absorption

ABSTRACT

Insufficiency of *Akkermansia muciniphila* (Akk) has been implicated in the pathogenesis of metabolic diseases, and administration or restoration of Akk has ameliorated these disorders. Recently, Pasteurized Akk (PA-Akk) has been approved as a functional food. However, the impact of Akk on lipid absorption in the proximal intestine, which is directly exposed to orally administered Akk, remains largely unexplored. In this study, we orally administered Akk and PA-Akk to mice and investigated the subsequent lipid absorption. Long-term administration of Akk resulted in reduced lipid deposits in the liver and adipocytes, along with improved glucose metabolism. This was primarily attributed to a reduction in lipid absorption by epithelial cells in the proximal jejunum. Mechanistically, Akk activated AMP-activated protein kinase (AMPK) and directly inhibit lipids absorption in both mouse and human jejunal epithelial cells. Furthermore, we demonstrated that Akk treatment, but not PA-Akk treatment, promotes the abundance of genera that are highly abundant in the normal jejunum and belong to the phylum Firmicutes. Thus, our study concludes that oral administration of Akk provides beneficial effects on metabolism, partially through inhibiting jejunal lipid absorption and promoting the abundance of core jejunal microbes.

1. Introduction

The gut microbiota plays a crucial role in maintaining host health. *Akkermansia muciniphila* (Akk), a bacterium that resides in the ileum and colon and feeds on mucins, has been identified as a promising next-generation probiotic. The deficiency of Akk in the gut has been associated with metabolic diseases such as obesity, type 2 diabetes (T2D), non-alcoholic fatty liver disease (NAFLD), and cardiovascular diseases (Everard et al., 2013; Santacruz et al., 2010; Karlsson et al., 2012; Zhang et al., 2013; Li et al., 2017). Studies have shown that promoting Akk growth or directly feeding Akk to obese and T2D mice can improve metabolic disorders, indicating a causal role of Akk in these conditions (Everard et al., 2013; Depommier et al., 2019). Pasteurized Akk can also improve metabolism in both mice and human, while little observed alteration in the gut microbiota (Everard et al., 2013; Depommier et al., 2019; Plovier et al., 2017). Although several components of Akk have been identified as contributing to host metabolism (Plovier et al., 2017; Yoon et al., 2021; Bae et al., 2022), the exhaustive signaling and molecular mechanism of the interaction between Akk and the host are still not fully understood.

The upper segments of the intestine, namely the distal duodenum and proximal jejunum, are the main areas responsible for dietary lipid digestion and absorption in the intestine. Numerous host cellular proteins involved in the regulation of lipid absorption have been identified in the duodenum and jejunum (Ko et al., 2020). However, the interaction between bacteria and epithelial cells in regulating lipid absorption

* Corresponding authors at: Institutes of Biomedical Sciences, College of Life Sciences, Inner Mongolia University, Hohhot, China.
E-mail addresses: tiemin_liu@fudan.edu.cn (T. Liu), shiqijia@jnu.edu.cn (S. Jia).
[1] 0000–0001-8595–9314

https://doi.org/10.1016/j.micres.2025.128053
Received 24 September 2024; Received in revised form 29 December 2024; Accepted 4 January 2025
Available online 6 January 2025

is not fully understood. This is primarily due to the relatively lower number of bacteria in the upper segments of the intestine compared to the colon, as well as the difficulty in accessing the small intestine in healthy humans, which has resulted in limited research on the bacteria in the small intestine (Lema et al., 2020). Nevertheless, one recent study has shown that Akk represses the expression of glucose transporters in the jejunum, highlighting the importance of the interaction between Akk and jejunal epithelia (Depommier et al., 2020).

AMPK is an evolutionarily conserved kinase that consists of a catalytic α subunit and regulatory β and γ subunits. AMPK is activated by increased ratios of AMP/ATP and ADP/ATP, as well as other signals. This activation involves the phosphorylation of AMPKα at Thr172 (Hardie et al., 2012). AMPK activation promotes ATP production by increasing the activity or expression of catabolic proteins, while conserving ATP by switching off biosynthetic pathways. Activation of duodenal AMPK by metformin activates a gut-brain-liver axis, which inhibits hepatic glucose production and lowers blood glucose levels (Duca et al., 2015). Additionally, activation of jejunal AMPK decreases the biogenesis of free fatty acids and lipoprotein and inhibits the activity of lipid synthesis enzymes, thus reducing the production of triglycerides, phospholipids, and cholesteryl esters (Harmel et al., 2014).

Given that the oral administration of Akk plays a crucial role in metabolic regulation, we hypothesized that Akk may exert its functions in the upper segments of the intestine. In this study, we demonstrated the function of both Akk and PA-Akk in regulating lipid absorption in the proximal jejunum.

2. Results

2.1. Oral administration of Akk promotes glucose and lipid metabolism in mice fed either a normal chow diet or a high-fat diet

To assess the effects of orally administrated Akk on mice fed a normal chow diet (ND), we administered 4 × 10^8 Akk and pasteurized Akk (PA-Akk) daily for seven weeks via gavage. We monitored glucose metabolism during the treatment to determine the appropriate time point, which was set at seven weeks (Fig. S1A,B). The bodyweight was comparable among the mice treated with PBS, Akk, and PA-Akk (Fig. 1A). However, both Akk and PA-Akk administration enhanced glucose tolerance and insulin sensitivity (Fig. 1B,C) and reduced blood triglyceride levels (Fig. 1D). Thus, both Akk and PA-Akk administration improve glucose metabolism and lower blood lipid levels in mice fed a normal chow diet.

The effects of Akk on high-fat diet (HFD)-fed mice were also explored based on a prolonged treatment period. Since 16 weeks of HFD feeding induce insulin intolerance and metabolic impairment in mice, we included 18 weeks of HFD feeding and Akk treatment in our analysis. We administrated 4 × 10^8 Akk and PA-Akk daily for 18 weeks to HFD-fed mice (Fig. 1E). We observed decreased body weight, improved glucose tolerance and insulin sensitivity in mice treated with Akk and PA-Akk (Fig. 1F,G,H,I). Notably, serum triglycerides and cholesterol levels were reduced in both Akk and PA-Akk treated mice (Fig. 1J,K). Thus, oral administration of Akk or PA-Akk ameliorates glucose and lipid metabolism and reduces serum lipid levels in HFD-fed mice.

Metabolic alterations in HFD-fed mice with or without Akk administration were further investigated using metabolic cage analysis. Energy expenditure was increased in Akk-treated mice but not in those receiving PA-Akk (Fig. 1L). Correspondingly, oxygen consumption and the carbon dioxide production were increased in Akk-treated mice but remained unchanged in PA-Akk-treated ones (Fig. 1M,N). However, the respiratory exchange ratio (RER), which is indicative of metabolic substrate utilization, was comparable across all groups (Fig. 1O). Increased nocturnal activity was unique to Akk-treated mice (Fig. 1P), whereas food consumption declined in both Akk and PA-Akk groups (Fig. 1Q). We measured the body temperature under both room temperature and cold stress conditions. Both orbital and rectal temperatures were increased in both Akk and PA-Akk treated mice in both conditions (Fig. 1R,S). In summary, Akk-treated mice exhibited higher energy expenditure, activity levels, and body temperature but consumed less food, while PA-Akk-treated mice displayed reduced food intake and increased body temperature.

2.2. Oral administration of Akk reduces lipid absorption in the proximal jejunum

The reduction of blood lipid levels and overall promotion of metabolism led us to investigate lipid absorption in the intestines of Akk-treated mice. In HFD-fed mice, we observed increased daily feces excretion in Akk-treated mice but little changes in PA-Akk-treated mice (Fig. 2A,B). Consequently, the daily fecal lipids excretion and the feeding lipids excretion were higher in the Akk-treated mice (Fig. 2C and Fig.S1C). Oil Red staining revealed reduced lipid content in the proximal jejunum of both Akk- and PA-Akk-treated mice (Fig. 2D). Additionally, portal vein triglyceride levels were lower following corn oil gavage in both Akk- and PA-Akk-treated mice (Fig. 2E). The oral lipid tolerance test (OLTT) demonstrated reduced lipid absorption following a lipid challenge in both Akk- and PA-Akk-treated mice (Fig. 2F). These data suggest reduced lipid uptake in the proximal jejunum of mice treated with either Akk or PA-Akk.

Eighteen-week HFD feeding led to hepatic lipid accumulation (Fig. 2G-I). Akk or PA-Akk treatment lessened liver weight (Fig. 2G), darkened liver color, reduced vacuolation in hepatocytes (Fig. 2H), and decreased hepatocytic lipid accumulation (Fig. 2I). However, HFD did not induce fibrosis in PBS-, Akk-, or PA-Akk-treated mice (Fig.S1D). Additionally, neither Akk nor PA-Akk administration elevated the levels of alanine aminotransferase (ALT) and aspartate aminotransferase (AST), which are considered inflammation markers in the liver (Fig.S1E, F). In adipose tissues, the size of adipocyte was decreased in both epididymal and inguinal fat (Fig. 2J,K, and Fig.S1G,H), accompanied by an overall reduction in fat weight in mice treated with either Akk or PA-Akk (Fig.S1I,J). We followed the mice for two months after the 18-week Akk treatment and measured body weight and lipid absorption. Both the Akk and PA-Akk groups maintained lower body weight (Fig.S1K) and reduced blood triglyceride levels before and after oil gavage compared to the PBS control group (Fig.S1L), indicating that the metabolic benefits persisted even after the Akk treatment was discontinued. In summary, Akk and PA-Akk treatments result in reduced lipid accumulation in the liver and adipose tissues.

2.3. Akk activates AMPK in epithelial cells of the proximal jejunum

To investigate how Akk regulates lipid absorption in the small intestine, we examined gene expression in intestinal epithelial cells using RNA-seq in PBS- and Akk-administered mice fed a normal chow diet. We identified 1273 dysregulated genes, including 296 upregulated and 977 downregulated genes, with a cutoff of p-value < 0.05 and fold change (FC)> 1.5 (Fig. 3A and Table S1). The dysregulated genes were confirmed by real-time quantitative reverse transcription PCR (qRT-PCR) (Fig. 3B). Gene set enrichment analysis (GSEA) revealed that the most significantly enriched gene sets were negatively associated with Ribosome, cell cycle, DNA replication and RNA polymerase (Fig. 3C and Table S2), indicating repression of biosynthesis following oral administration of Akk. Among these genes, the expression of *Fasn* and *Acc1 (Acaca),* which regulate lipid neogenesis and are targets of AMPK signaling, was downregulated (Fig. 3A,B). Given that activation of AMPK can trigger the repression of energy expenditure such as the repression of proliferation and biosynthesis as observed in our GSEA analysis (Hardie et al., 2012), we further examined AMPK activity by detecting phosphorylation of AMPKα (Thr172). Administration with either Akk or PA-Akk increased the phosphorylation of AMPKα and reduced the expression of AMPK targeted genes *Fasn* and *Acc1* in the proximal jejunum epithelial cells of mice fed a HFD (Fig. 4A,B). Thus,

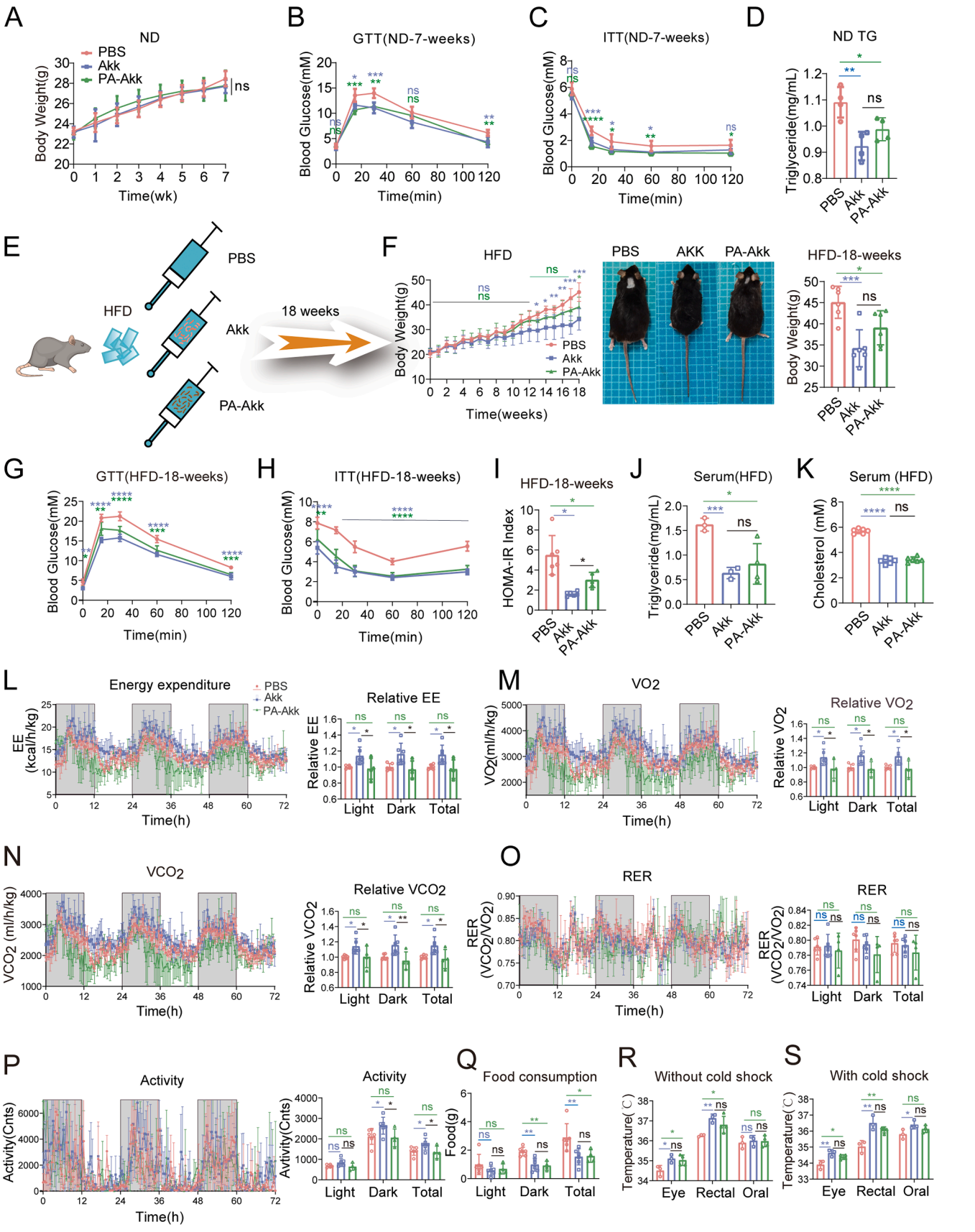

(caption on next page)

Fig. 1. Effects of orally administrated Akk on metabolism in mice fed either a normal chow diet or a high-fat diet. Mice fed a normal chow diet were orally administered PBS, Akk or PA-Akk for 7 weeks. (A) body weight, (B) glucose tolerance, (C) insulin tolerance, and (D) blood triglyceride levels were measured (n = 4). (E) Schematic of PBS, Akk and PA-Akk administration to mice fed a high-fat diet. (F) Body weight, (G) glucose tolerance, (H) insulin tolerance, (I) Homeostasis Model Assessment for Insulin Resistance (HOMA-IR), (J) blood triglycerides, and (K) blood cholesterol were shown. Animal number n = 6 for (F-I and K) and n = 3–4 for (J). After 24 hours of acclimatization in metabolic cages, the HFD-fed mice underwent continuous metabolic monitoring over three days, including (L) energy expenditure (EE), (M) O2 consumption (VO2), (N) CO2 production (VCO2), (O) respiratory exchange ratio (RER), (P) physical activity, and (Q) food intake. Experiments were conducted after 18 weeks of HFD feeding and oral administration of PBS, Akk, and PA-Akk. Bar graphs represent mean values from three consecutive days and nights, normalized to those of PBS-treated mice (A-C) or shown as counts (D-H), animal number n = 4–6. Temperatures were measured from the eye, rectal, and oral positions under (R) ambient and (S) cold stress conditions, animal number n = 3–4. Data are represented as mean ± SD; one-way analysis of variance (ANOVA) was used for comparisons among three groups, followed by Fisher's Least Significant Difference test for post-hoc multiple comparisons. ns, not significant; p > 0.05, * or # p < 0.05, **p < 0.01, * **p < 0.001, * ** *p < 0.0001. Significance of Akk vs PBS and PA-Akk vs PBS is shown in blue and green color, respectively.

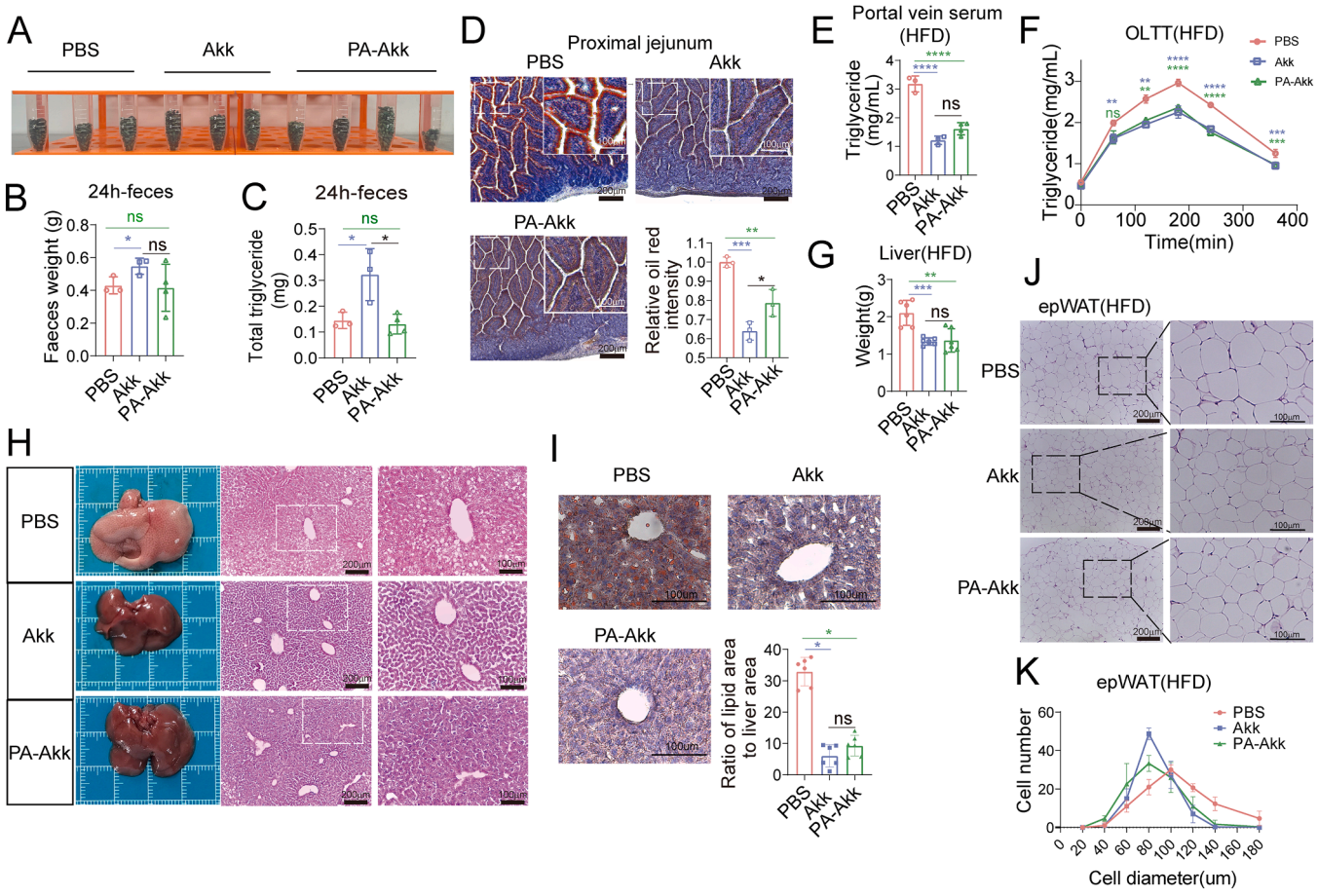

Fig. 2. Lipid absorption, excretion and accumulation in the mice fed a HFD and administrated PBS, Akk and PA-Akk for 18 weeks. (A-C) 24-hour feces (A,B) and fecal triglyceride levels (C) collected from the mice fed a HFD, animal number n = 3–4. (D) Oil Red O staining of lipid content in jejunal villi and (E) portal vein blood triglyceride levels. Gavage of PBS, Akk and PA-Akk was performed 2 hours before dissection, followed by corn oil gavage (10ul/g body weight) 1 hour later. The distal jejunum was collected for staining, and portal vein blood was collected for lipid measurements, animal number n = 3 for each group. (F) Oral Lipid Tolerance Test (OLTT) analysis in the mice that fed a HFD and administrated PBS, Akk and PA-Akk for 18 weeks. Animal number n = 4, statistical significance is shown as Akk vs PBS (blue) and PA-Akk vs PBS (green) respectively. (G-I) Liver weight (G), liver appearance and H&E staining (H), and liver Oil Red O staining (I) are shown. (J-K) H&E staining of epididymal fat (J) and quantification of adipocyte size (K), animal number n = 6. Data are presented as mean ± SD. One-way analysis of variance (ANOVA) was used for comparisons among three groups, followed by Fisher's Least Significant Difference test for post-hoc multiple comparisons. ns, p > 0.05, *p < 0.05, * *p < 0.01, * **p < 0.001, * ** *p < 0.0001.

Akk promotes AMPK activation in the mouse jejunum.

We next explored the regulatory role of Akk on AMPKα phosphorylation and lipid absorption using an in vivo incubation method, in which the jejunum was incubated with the fluorescence labelled lipid Bodipy-C12 in the presence of various stimulators. First, we tested the incubation system using the AMPKα activator metformin and the inhibitor compound C. Metformin promoted the phosphorylation of AMPKα and repressed Bodipy C12 absorption, while Compound C did not further inhibit the phosphorylation of AMPKα in the presence of lipids but promoted Bodipy-C12 absorption (Fig.S2A-D). Next, we test Akk function using this method. Akk enhanced the phosphorylation of AMPKα, while metformin did not further increase the Akk induced phosphorylation levels (Fig. 4C). Conversely, compound C eliminated the phosphorylation induced by Akk (Fig. 4C). Correspondingly, we detected a significant reduction in Bodipy-C12 absorption in the presence of Akk (Fig. 4D, E). Although metformin did not further reduce Bodipy-C12 levels in Akk-treated villi, compound C reversed the impact of Akk and restored Bodipy-C12 absorption in the villi (Fig. 4D,E). These results demonstrated that Akk inhibits lipid absorption through the activation of the AMPK pathway.

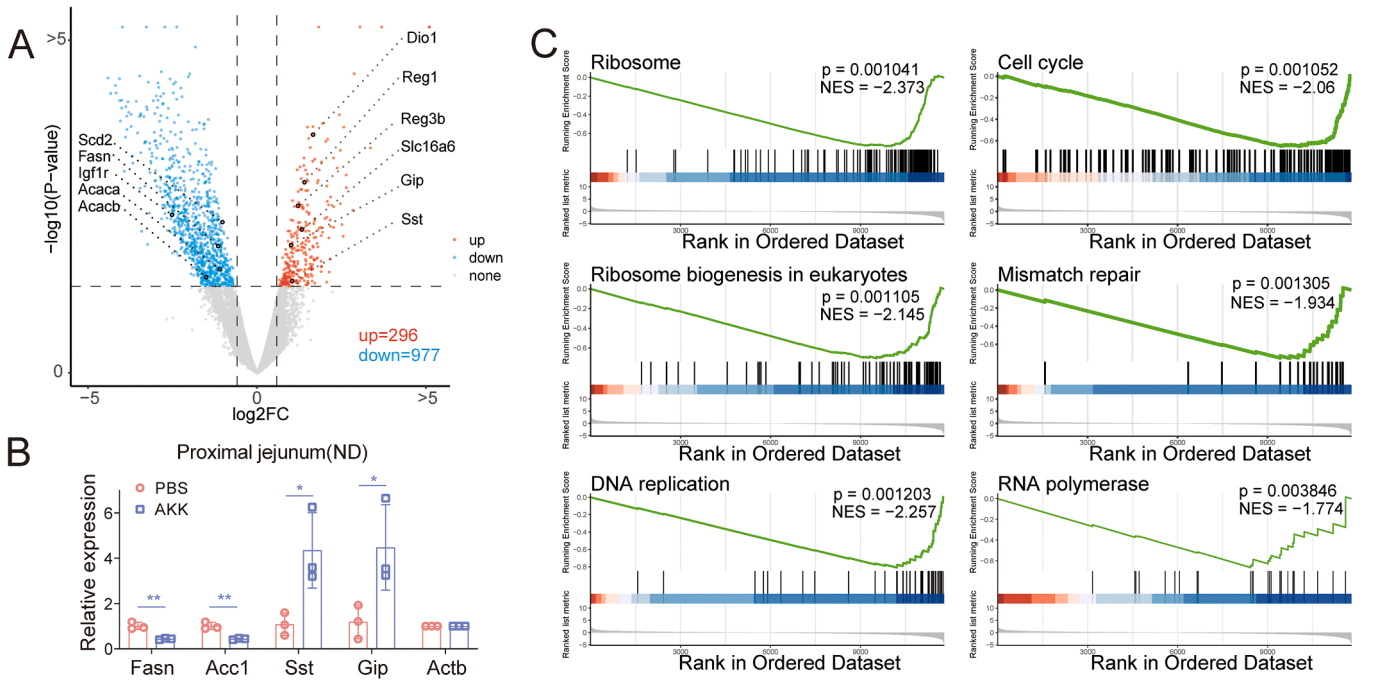

Fig. 3. Gene expression in intestinal epithelial cells. (A) Volcano plot showing differentially expressed genes in small intestinal epithelial cells of Akk-administrated mice, n = 3 for each group. (B) qRT-PCR verification of differentially expressed genes in intestinal epithelia of Akk-administrated mice, animal number n = 3. (C) GSEA demonstrating enriched pathways in intestinal epithelial cells of the Akk-treated mice, including ribosome, cell cycle, ribosome biogenesis, mismatch repair, DNA replication, and RNA polymerase pathways. qRT-PCR data are presented as mean ± SD. Comparisons between two groups were analyzed using Student's *t*-test. *p < 0.05, * *p < 0.01.

Next, we investigated the effect of Akk on human jejunal epithelial cells by employing an ex vivo incubation method, in which freshly isolated jejunum was incubated with various stimulators. We verified the responses of AMPKα phosphorylation and lipid absorption to metformin and compound C (Fig.S2E-H) and the regulation of AMPKα phosphorylation by Akk but not E.coli (Fig. 5A) in human jejunal epithelial cells. We detected that Akk prompted the phosphorylation of AMPKα and decreased fluorescence-labeled lipid absorption (Fig. 5B,C). Metformin did not further enhance the effects of Akk on AMPKα phosphorylation or lipid absorption, while the AMPK inhibitor compound C inhibited Akk function (Fig. 5B,C). These data indicated that Akk activates the AMPK pathway and inhibits lipid absorption in the human proximal jejunum.

2.4. *Akk promotes jejunal core bacteria*

As little is known about the effects of Akk on jejunal microbiota, we investigated whether Akk or PA-Akk administration effects jejunal resident bacteria. To this end, we collected jejunal epithelial contents from mice administrated with PBS, Akk and PA-Akk and performed 16S rRNA sequencing. To avoid detecting the administrated Akk, we stopped Akk and PA-Akk administration one day before dissection. We found that Akk administration decreased the richness of jejunal microbiota but did not change its evenness, as assessed by Chao (Chao, 1984) and Shannon (Shannon, 1948) indices, while PA-Akk had no effect on the richness and evenness of jejunal microbes (Fig. 6 A,B). Furthermore, principal component analysis (PCA) revealed that the types and abundance of jejunal microbes were significantly altered in Akk-treated mice but not in PA-Akk-treated mice (Fig. 6 C). These data indicate that Akk treatment alters the structure of jejunal microbiota.

We analyzed the differentially abundant bacteria at the genus level in the jejunum among PBS, Akk, and PA-Akk treatments. Although some bacteria decreased or were lost, Akk treatment particularly promoted the abundance of genera that are highly abundant in the normal jejunum and belong to the phylum Firmicutes (Fig. 6D-G and Table S3 and S4). These genera include *Candidatus Arthromitus, Dubosiella, Ileibacterium, Faecalibaculum,* and *Microbacterium* (Table S4). *Candidatus Arthromitus* was the most abundant genus induced by Akk treatment, accounting for 23.2 ± 6.3 % of the jejunal microbes in Akk-treated mice, compared to 0.025 ± 0.017 % in PBS-treated mice and 0.69 ± 0.68 % in PA-Akk-treated mice (Fig. 6D, Table S4). However, the abundance of Akk itself was very low in the jejunum, at 0.018 ± 0.0094 % in PBS-treated mice, and there was no increase in mice treated with Akk or PA-Akk (Fig. 6H). Thus, oral administration of Akk alters the jejunal microbiota and promotes jejunal core bacteria.

3. Discussion

Akk has been characterized as a next generation probiotic that benefits host metabolism and inhibits inflammation. Previous works have shown that Akk inhabits the distal part of the intestine and colon, where it improves host metabolism by digesting mucin, enhancing intestinal barrier function, generating metabolic factors, and supporting a healthy microbiota (Cani et al., 2022). Oral administration of either live or pastured inactive Akk has been found to alleviate metabolic disorders in T2D/obese animals and overweight/obese patients (Everard et al., 2013; Depommier et al., 2019; Plovier et al., 2017). This raises the question of whether orally ingested Akk may function in ways beyond directly residing or acting in the distal intestine and colon to achieve therapeutic effects in these diseased subjects. For instance, orally administrated Akk passes through and is mostly digested in the upper segments of the intestine, where the majority of the glucose and lipid absorption occurs. Despite this, it still exerts beneficial effects on metabolism, possibly by functioning in the jejunum and modulating the jejunal microbial composition.

3.1. *Akk inhibits jejunal lipid absorption*

We demonstrated that oral administration of live Akk did not increase Akk abundance in the colon of ND-fed animals. However, these animals demonstrated improved glucose metabolism and decreased

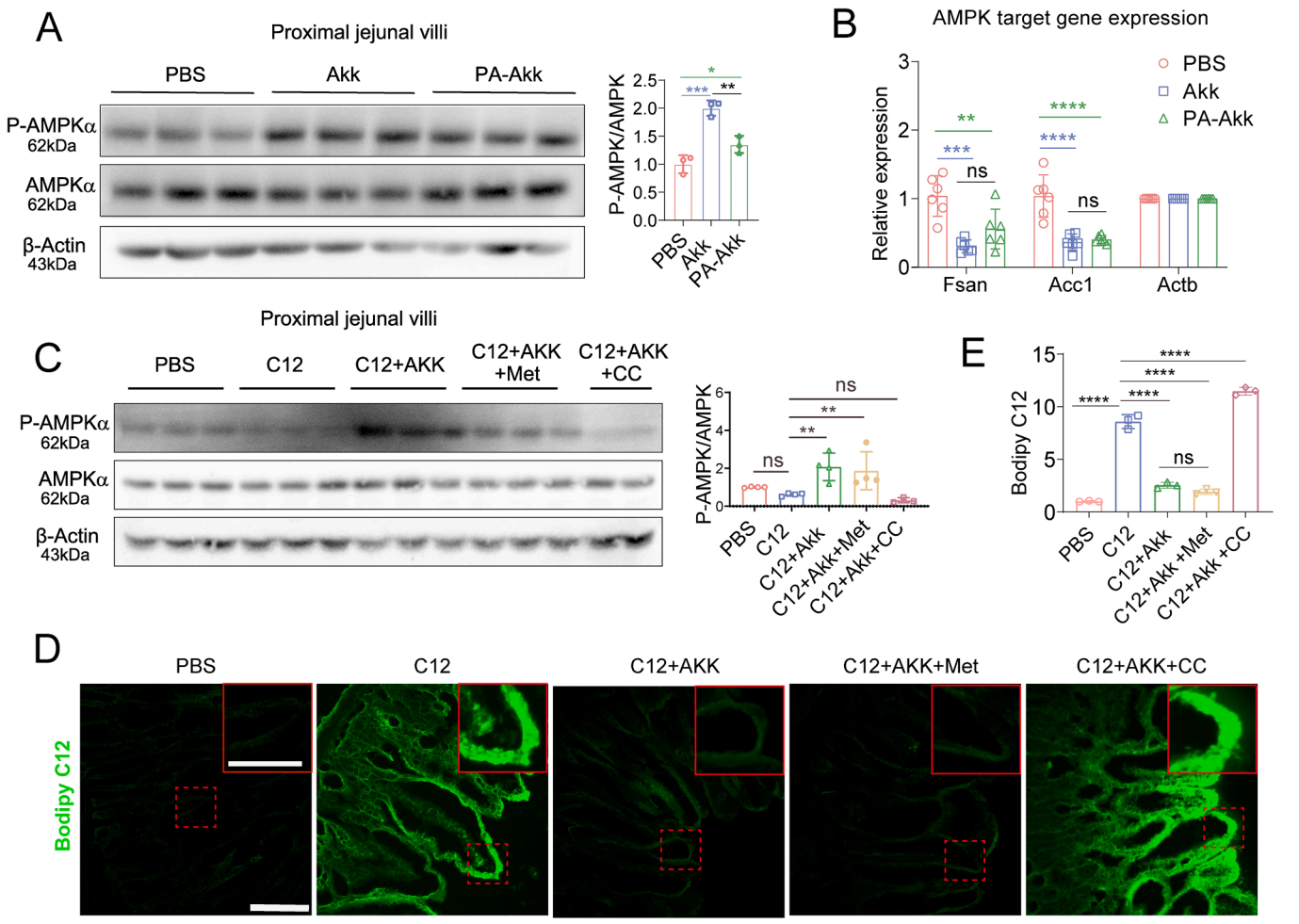

Fig. 4. Akk induces AMPK phosphorylation and modulates lipid absorption in mouse jejunal epithelial cells. (A) Western blot analysis of AMPKα phosphorylation levels in the proximal jejunum epithelial cells of HFD-fed mice administrated PBS, Akk and PA-Akk. Quantification of phosphorylated-AMPKα/AMPKα is shown on the right panel, with beta-Actin as a loading control. Animal number n = 3 for each group. (B) Expression of AMPK target genes analyzed by qRT-PCR in the proximal jejunal epithelia of HFD-fed mice, animal number n = 6 for each group. (C-E) Analysis of AMPKα activity and intestinal lipid absorption in jejunum. (C) Western blot analysis of jejunal villi using antibodies against phosphorylated AMPKα, AMPKα, and beta-actin in each indicated treatment. Quantification of p-AMPKα vs AMPKα is shown on the right panel. (D) Immunofluorescence showing absorption of fluorescence-labeled fatty acid Bodipy-C12. Scale bar shows 50 μm and 25 μm in the main and magnified panels, respectively. (E) Quantification of fluorescence intensity from (D), animal number n = 3 for each group. Data are presented as mean ± SD. One-way analysis of variance (ANOVA) was used for comparisons among multiple groups, followed by Fisher's Least Significant Difference test for post-hoc multiple comparisons. ns, $p > 0.05$, *$p < 0.05$, * *$p < 0.01$, * **$p < 0.001$, * *** *$p < 0.0001$.

blood lipid levels. To explore novel models of Akk function, we conducted the gene expression and lipid absorption analysis in the intestine. We found that Akk inhibited lipid absorption in the jejunum, a process regulated by the activation of AMPK. AMPK activation not only suppresses the expression of de novo lipogenesis gene *Acc1* and *Fasn* but also directly inhibits lipid absorption. Therefore, we showed for the first time that Akk can induce AMPK phosphorylation and contribute to the inhibition of lipid neogenesis and absorption in mice. In human jejunum, we observed the same regulatory role of Akk in activating AMPK and inhibiting lipid absorption. Thus, we proposed that orally administered Akk interacts with epithelial cells in the proximal jejunum, activates AMPK pathway, and inhibits lipid absorption. Our data provide a new perspective on Akk function and suggest a novel mechanism for Akk-based therapeutic interventions in treating or preventing metabolic diseases.

3.2. *Akk but not PA-Akk promotes the abundance of core jejunal bacteria*

We identified that live Akk more significantly inhibits lipids absorption than pasteurized inactive Akk in the jejunum in vivo. Firstly, jejunal epithelial cells contained fewer lipids in Akk-fed mice compared to PA-Akk-fed mice. Secondly, we detected increased daily feces and lipid excretion in mice fed Akk but not those fed PA-Akk. Nevertheless, no significant difference was found in glucose metabolism and lipid accumulation in liver and adipocytes between Akk and PA-Akk treated mice, and no difference was observed in acute lipid absorption between the two groups. Plovier, H et al. observed greater glucose metabolic benefits in Akk treated HFD mice compared to PA-Akk treated HFD mice (Plovier et al., 2017). Meanwhile Depommier, C et al. found that PA-Akk improved liver function and inflammation better than Akk in treating obese/overweight humans (Depommier et al., 2019). However, the data also indicated a trend of lower triglyceride levels in live Akk-administered obese/overweight humans (Depommier et al., 2019). To date, the specific differences in metabolic regulation between Akk and PA-Akk are not well understood. Here we showed that although both Akk and PA-Akk promote AMPK activity in jejunal villi, they have different effects on modifying the jejunal microbiota. Specifically, live Akk, but not PA-Akk, increased the abundance of several jejunal bacteria which belong to the main types of residents in the jejunum (Yan et al., 2022; Lkhagvaet al. 2021; Wang et al., 2019a). Among them, *Candidatus_Arthromitus,* which is believed to be beneficial in regulating inflammation and lipid metabolism (Chen et al., 2022; Tung et al., 2022; Ma

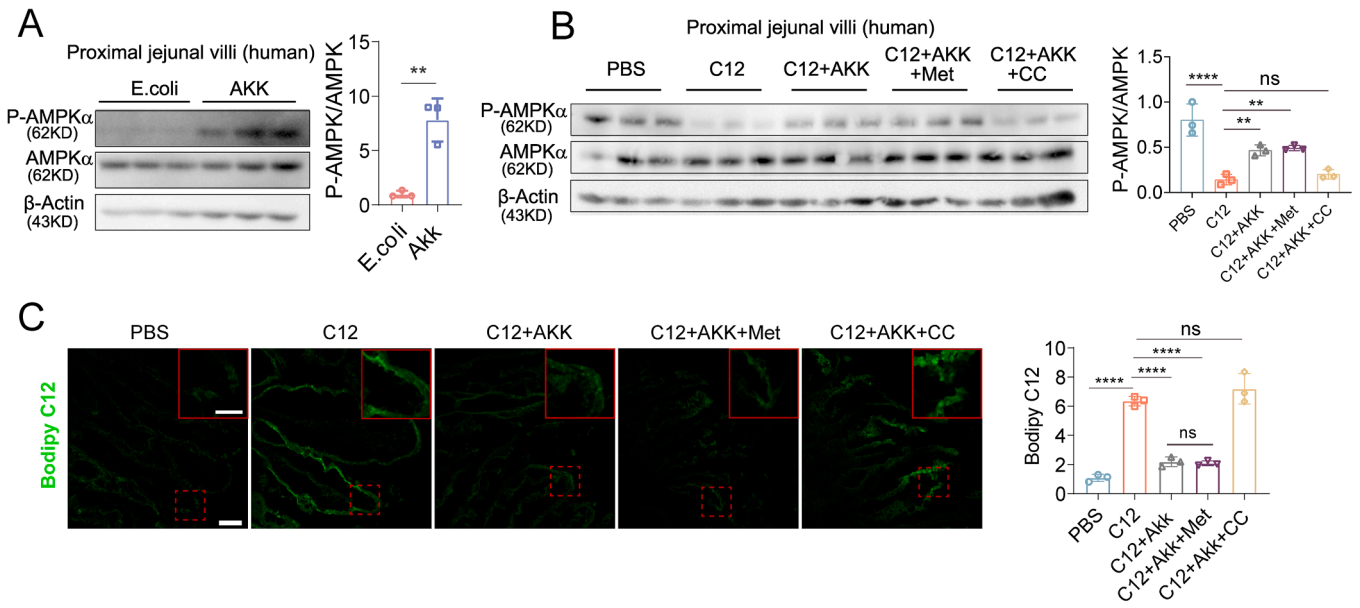

Fig. 5. Akk induces AMPK phosphorylation and modulates lipid absorption in human jejunal epithelial cells(A) Western blot analysis of phosphorylated AMPKα, AMPKα, and beta-Actin in human jejunal epithelial cells treated with E. coli and AKK. Quantification of phosphorylated-AMPKα/AMPKα is shown on the right panel, n = 3. (B-C) AMPKα phosphorylation and lipid absorption in human jejunum. PBS, Bodipy-C12, Bodipy-C12 plus Akk, Bodipy-C12 plus Akk and metformin, and Bodipy-C12 plus Akk and compound C were incubated with freshly collected human jejunal samples for 10 minutes. (B) Western blot analysis of jejunal villi using antibodies against phosphorylated AMPKα, AMPKα and beta-Actin. Quantification of phosphorylated-AMPKα/AMPKα is shown on the right panel. (C) Immunofluorescence analysis of Bodipy-C12 absorption in human jejunum, quantification analysis is shown on the right panel. Scale bar shows 50 μm and 25 μm in the main and magnified panels, respectively. Sample number n = 3 for each group. Data are presented as mean ± SD. Comparisons between two group were analyzed using Student's *t*-test. One-way analysis of variance (ANOVA) was used for comparisons among multiple groups, followed by Fisher's Least Significant Difference test for post-hoc multiple comparisons. ns, $p > 0.05$, *$p < 0.05$, * *$p < 0.01$, * **$p < 0.001$, * ** *$p < 0.0001$.

et al., 2019), increased nearly one-thousand-fold in response to Akk treatment. HFD treatment altered the composition of the microbiota, and specifically eliminated the intestinal *Candidatus_Arthromitus* (Tomas et al., 2016), indicating *Candidatus_Arthromitus* is negatively correlated with dietary fat and its abundance can be promoted by Akk. *Candidatus_Arthromitus* is reported to modulate the maturation of the host gut immune barrier (Schnupf et al., 2013, 2015) and thus plays an importance role in regulating intestinal function. Additionally, *Dubosiella*, a potential probiotic, contributes to the immune tolerance and protection against non-alcoholic fatty liver disease (NAFLD) and aging-related diseases (Chen et al., 2024; Zhang et al., 2024; Liu et al., 2023; Ye et al., 2023). Other Akk-regulated bacteria, such as *Ileibacterium*, *Faecalibaculum*, and *Microbacterium*, are also considered potential probiotics (Wang et al., 2022; Nagarajan et al., 2024; Cao et al., 2024; Guo et al., 2023). Therefore, we conclude that live Akk promotes the abundance of core jejunal bacteria and contributes to additional metabolic effects in the host. Further functional investigation of these jejunal bacteria is needed.

3.3. Akk activates AMPK signaling pathway

Metformin is used to treat T2D through various mechanisms, one of the main mechanisms being the activation of AMPK pathway (Rena et al., 2017). Interestingly, metformin can also promote Akk growth in vivo (de la Cuesta-Zuluaga et al., 2017; Shin et al., 2014). We showed that Akk, metformin, and the combination of Akk plus metformin can active AMPK in the jejunum and inhibit lipid absorption with comparable intensities, indicating a common pathway and overlapping functions between Akk and metformin in regulating lipid metabolism in the jejunum. Further investigation into whether Akk functions similarly to metformin by regulating AMPK in multiple other tissues would be interesting.

Overall, the total number of animals used in this study was large, and the experiments were conducted in several batches. However , the number of animals in each individual experiment was not sufficiently large. Nevertheless, statistical significance was observed in these experiments.

4. Conclusion

Our data showed that orally administered Akk or PA-Akk promoted AMPK activity and inhibited lipid absorption in the proximal jejunum. Furthermore, Akk treatment, but not PA-Akk, increased the abundance of core jejunal bacteria, which further contribute to the metabolic benefits of Akk administration. Overall, oral administration of Akk decreased lipid accumulation in the liver and adipocytes and improved insulin sensitivity and glucose metabolism.

Our findings highlight the upper segments of the intestine as a critical site of interaction with ingested Akk and uncover novel functions of Akk in regulating AMPK activity to inhibit lipid absorption and modulating the jejunal microbiota.

Our study suggests that oral administration of Akk has the potential to treat obesity and lipid disorders in human patients. Considering the reduced food intake, decreased lipid absorption, lowered blood triglycerides and cholesterol, and increased lipid excretion observed in mice, taking Akk could be an effective way to reduce lipid accumulation, which is particularly significant for individuals consuming high-fat Western diets. However, the exact effects need to be examined and verified through further clinical trials.

5. Materials and methods

5.1. Animals

Adult male C57/BL6N mice (8 weeks old) were used. The mice were fed either a normal chow diet (ND) or a high fat diet (HFD) (D12492, Research Diets). with ad libitum access to food throughout a 12-hour light/dark cycle at a controlled temperature of 21–23°C. Akk or

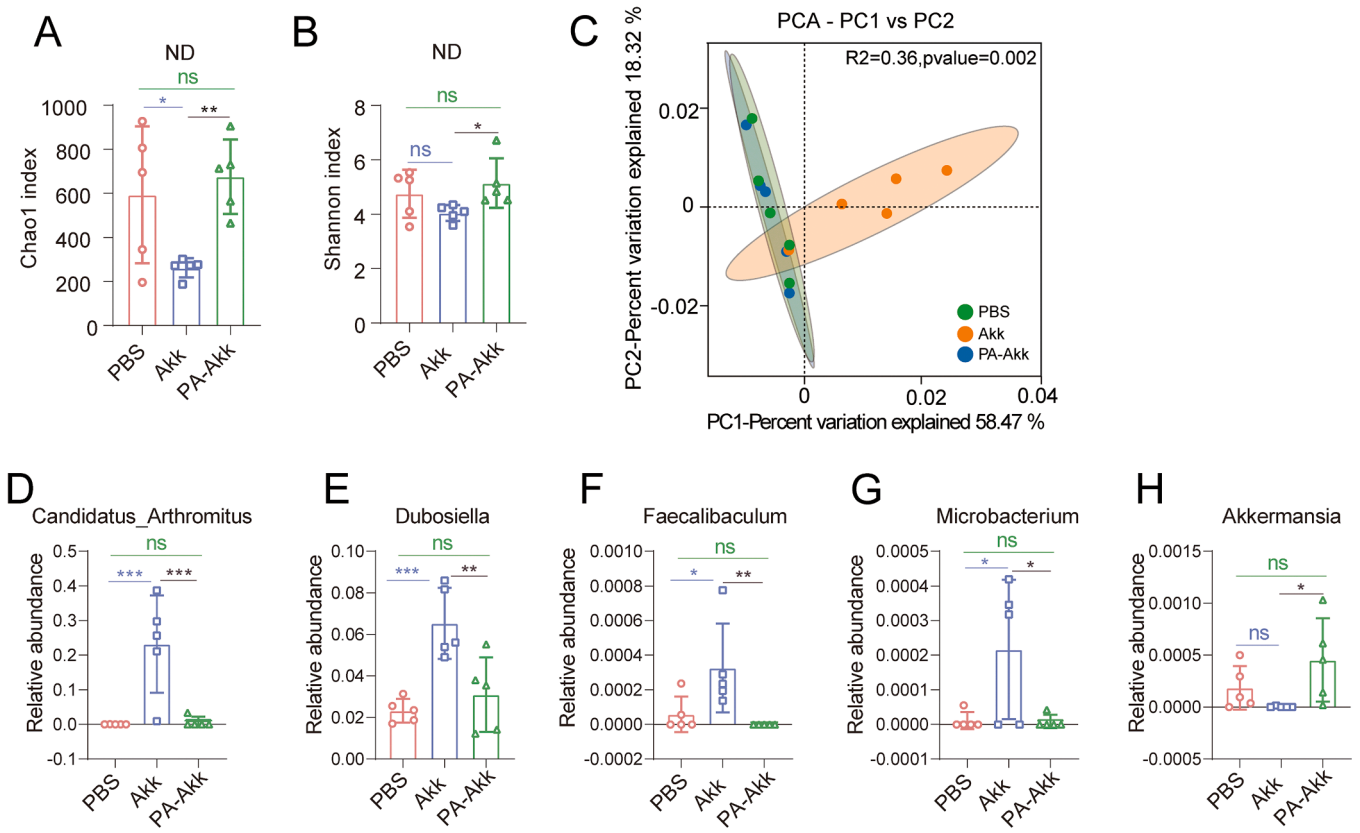

Fig. 6. 16S rRNA gene sequencing analysis of jejunal bacteria in ND-fed mice. (A, B) Chao and Shannon index showing the alpha diversity of gut microbiota in PBS, Akk and PA-Akk treated ND-fed mice. (C) PCA plot showing the beta diversity of gut microbiota in PBS, Akk and PA-Akk treated ND-fed mice. (D-H) Relative abundance of Candidatus_Arthromitus (D), Dubosiella (E), Faecalibaculum (F), Microbacterium (G), and Akkermansia (H) in jejunal collections from mice administrated PBS, Akk and PA-Akk for 7-week with a normal diet. Animal number n = 5. Data are presented as mean ± SD. One-way analysis of variance (ANOVA) was used for comparisons among three groups, followed by Fisher's Least Significant Difference test for post-hoc multiple comparisons. ns, $p > 0.05$, *$p < 0.05$, * *$p < 0.01$, * **$p < 0.001$.

pasteurized Akk were orally administered via gavage at a dose of 4 × 10^8 per day. The treatment duration was seven weeks for ND-fed mice and eighteen weeks for HFD-fed mice. For the preparation of active Akk, cultured Akk was collected, aliquoted, and frozen. For PA-Akk, Akk was collected and pasteurized in PBS at 70°C for 30 minutes to kill the bacteria. Animal experiments were approved by the Institutional Animal Care and Use Committee of the Jinan University (IACUC-20231225–05).

5.2. Culture of Akkermansia muciniphila

Akk (ATCC-BAA-835) was cultured with modifications to previously described methods (Yoon et al., 2021; Derrien et al., 2004). Briefly, Akk was cultured in anaerobic incubator (LAI-3T, LONGGYUE, China) for 48 hours in a media containing various nutrients, 13 g/L soyabean peptone, 5 g/L tryptone,17.5 g/L brain heart infusion broth, 5.5 g/L N-acetylglucosamine, 1.4 g/L Na2HPO4, 4 g/L threonine, 2.8 g/L NaCl, 1 g/L glucose, and 0.5 g/L L-cysteine monohydrochloride. Post-culture, Akk was centrifuged at 4000 g for 10 minutes, washed, and resuspended in 20 % glycerol/PBS at a concentration of 2 × 10^9/ml. Each mouse received 200ul per day. Pasteurization was performed at 70ºC for 30 minutes, and verification of no living Akk was conducted through clonal culture. The same amount of PA-Akk was used in the treatments administered to mice as active Akk.

5.3. Glucose tolerance test and insulin resistance test

Glucose tolerance tests (GTT) were carried out following established protocols (Tao et al., 2018). Mice were fasted overnight and subsequently received an intraperitoneal (IP) injection of glucose at a dose of 2 g/kg body weight. Tail blood glucose levels were measured at predetermined time points (0, 15, 30, 60, and 120 minutes) post-injection using a Sinocare glucometer (GA-3). Similarly, insulin resistance tests (ITT) were conducted as described previously (Tao et al., 2018), with mice fasted for 6 hours and receiving an IP injection of insulin (I9278, Sigma, USA) at a dose of 0.375 U/kg body weight. Glucose levels were monitored within the same framework as GTT. Homeostatic model assessment-insulin resistance (HOMA-IR) was calculated using the insulin and glucose levels obtained from 16-hour fasted mice according to the formula, HOMA-IR = [insulin (μU/ml) x glucose (mM)] / 22.5 (Gawlik et al., 2020)

5.4. Blood and fecal triglyceride measurement

For blood triglyceride analysis, blood was drawn from retro-orbital plexus of fasted mice. An oral lipid tolerance test (OLTT) was conducted as described (Ochiai, 2020). Briefly, mice were fasted overnight (12-hour) and subsequently fed with corn oil at a dose of 5 ml/kg body weight. Blood was drawn before and at 1, 2, 3, 4, and 6 hours after oil administration. For portal vein triglyceride measurement, mice were orally administered with PBS, Akk or PA-Akk, followed by a corn oil gavage (10ul/g body weight) one hour later. Portal vein blood was collected one hour after oil gavage. Blood samples were allowed to clot and were then centrifuged to collect sera. Triglyceride levels were measured using a triglyceride assay kit (AKFA003M. Boxbio. China). For 24-hour fecal triglyceride measurements, 24-hour feces were collated

for each mouse over three consecutive days. The feces were weighted and triglyceride levels were measured accordingly. To test the excretion of feeding lipids, mice were fasted for 16 hours and then fed a HFD solution (3:1 in PBS) via gavage at a dose of 10 ml/kg body weight. Feces were collected over the following 6 hours and the fecal triglyceride levels were measured using the same kit.

5.5. 16S rRNA gene sequencing

Jejunal sample were collected from mice treated with PBS, Akk or PA-Akk for seven weeks. Mice were not administrated Akk or PA-Akk one day before dissection, and the jejunum was gently rinsed in PBS before collecting epithelial contents to avoid detecting orally administered Akk. Jejunal epithelial contents were collected with a rubber scrapper, snap-frozen in liquid nitrogen, and started at −80°C until bacterial DNA isolation. 16S rRNA library preparation and sequencing were performed as previously described (Chen et al., 2020). The sequencing data were analyzed using the BMKCloud platform (https://www.biocloud.net/).

5.6. RNAseq and qRT-PCR

Total RNA was isolated from epithelial cells scraped from the entire small intestine, and RNA-seq libraries were constructed and sequenced following previously established protocols (Liang et al., 2021). The BMKCloud platform was employed for subsequent data analysis (https://www.biocloud.net/). For qRT-PCR, RNAs were reverse transcript into cDNA, and primers listed in supplemental Table S5 were utilized.

5.7. Hematoxylin and eosin staining (H&E)

Liver and various adipose tissues were fixed in 4 % PFA for 24 hours. The tissues were dehydronated and embedded in paraffin as described previously (Liang et al., 2021). H&E staining procedures were followed as previously described (Tao et al., 2023).

5.8. Oil red O staining

Liver and intestine were fixed in 4 % PFA for 24-hour and then cryo-embedded. For Oil red O staining, slides were briefly rinsed in water and incubated with 60 % isopropanol for 1 minute, followed by incubation in 0.5 % Oil Red O for 10 minutes. This was succeeded by a 10-second 60 % isopropanol rinse and a 10-second nuclear hematoxylin stain. Finally, slides were washed in water for 1 minute before being coverslipped.

5.9. Western blot

Western blot was performed with slight modifications to previously established methods (Jia et al., 2015). Briefly, intestine villi were scrapped, lysed with RIPA buffer containing a proteinase inhibitor (4693159001, Rohe, Switzerland), and protein concentrations were determined using BCA assays (Beyotime,P0010, China). Primary antibodies used included phospho-AMPKalpha (Thr172) (2535S, CST, 1:1000) , AMPKalpha (2532S, CST, 1:1000), and ActB (GTX109639, GeneTex, 1:5000). For secondary detection, HRP-labeled anti-Rabbit IgG (H+L) (711–035–152, Jackson lab, 1:5000) was used. Imaging was carried out using an ImageQuant Minichemi 610 chemiluminescence imager (SageCreation, China).

5.10. PhenoMaster analysis

A PhenoMaster system (TSE Systems, Germany) was used to assess metabolic parameters, activity, and feeding and drinking behavior of mice. Each mouse was acclimatized to the metabolic cage for 24 hours before data collection over the following 72 hours. Groups of 4–6 mice were used for each experimental condition. Oral, rectal, and orbital temperatures were recorded using an animal thermometer (FT3400, KEW, China). To induce thermogenic stress, mice were individually housed in a cage at 4°C for 6 hours.

5.11. Lipid absorption analysis

In vivo intestinal lipid absorption was assessed as follows: mice were pre-treated with PBS, Akk, Akk plus metformin, or Akk plus compound C one hour prior to the experiment. Then the mice were anesthetized as described previously (Wang et al., 2019b). The proximal jejunum, located 10 cm to 20 cm distal to the pylorus, was clamped off for incubation. The isolated segment was filled with 1 ml of either PBS or a 2uM final concentration of Bodipy-C12 (molecular probes, D3823, ThermoFisher, USA) and incubated for 10 minutes. The jejunum was then collected for either immunohistology analysis or Western blot testing.

5.12. Lipid absorption in human intestine

Human proximal jejunum samples were obtained from patients undergoing bariatric surgery. One-centimeter length of jejunal segments were taken from the intestine located 50 cm distal to the ligament of Treitz. The specimens were incubated for 10 minutes with various compounds, including Escherichia coli (E.Coli), Akk, PBS, Bodipy-C12, and combinations of Bodipy-C12 with Akk, metformin, or compound C. The specimens were processed post-incubation for immunohistology and the villi were isolated for Western blot analysis. Informed consent for sample donation was obtained, and all procedures involving human tissue were authorized by the Institutional Review Board (IRB) of the First Affiliated Hospital of Jinan University (KY-2023–229).

5.13. Statistical methods

Statistical analyses were conducted using Prism 9 software (GraphPad Software, San Diego, CA) or Microsoft Excel. An unpaired Student's *t*-test was used to compare two distinct groups. For comparisons involving three or more groups, one-way analysis of variance (ANOVA) was employed, followed by Fisher's Least Significant Difference test for post-hoc multiple comparisons. A p-value of less than 0.05 was considered statistically significant. Results were presented as mean ± standard deviation. For the quantification of immunofluorescence, Western blot band intensities, and Oil Red O staining, Image J software was used.

Fundings

This work was supported by the Guangzhou Science and Technology Program (2023A03J1017), the Natural Science Foundation of Guangdong Province-General Program (2023A1515011077), the Clinical Frontier Technology Program of the First Affiliated Hospital of Jinan University (JNU1AF-CFTP-2022-a01236), and Inner Mongolia University "Steed Plan" high-level talent funding (10000–23122101/029).

Author statement

Q.M. performed the experiments and prepared the figures. X.Z., W.S., and Q.W. contributed to the animal experiments, bacterium preparation, and sample collection. G.Y. contributed to the bacterium culture. W.T. contributed to the sample collection and conservation. Z.D. and C. W. contributed to the human tissue collection. C.W. and T.L. contributed to the critical discussion of the experiments and the data. S.J. supervised the project, organized the data, and wrote the manuscript.

Author contributions

Q.M. performed the experiments and prepared the figures. X.Z., W.S.

and Q.W. contributed to the animal experiments, the bacterium preparation, and sample collection. G.Y. contributed to the bacterium culture. W.T. contributed to the sample collection and conservation. Z.D. and C. W. contributed to the human tissue collection. C.W. and T.L. contributed to the critical discussion of the experiments and data. S.J. supervised the project, organized the data, and wrote the manuscript.

CRediT authorship contribution statement

Weikang Su: Validation, Methodology. **Qingyu Wang:** Resources, Methodology. **Guoxing Yu:** Software, Data curation. **Weihua Tao:** Visualization, Validation, Resources. **Shiqi Jia:** Writing – review & editing, Writing – original draft, Supervision, Project administration, Funding acquisition, Conceptualization. **Qiming Ma:** Visualization, Software, Resources, Project administration, Methodology, Formal analysis. **Xincheng Zhou:** Visualization, Validation, Methodology. **Zhiyong Dong:** Conceptualization. **Cunchuan Wang:** Resources. **Chi-Ming Wong:** Conceptualization. **Tiemin Liu:** Conceptualization.

Declaration of Competing Interest

The authors report there are no competing interests to declare.

Acknowledgments

We thank the Biobank of the First Affiliated Hospital of Jinan University for assistance in the collection and preservation of human intestine materials.

Appendix A. Supporting information

Supplementary data associated with this article can be found in the online version at doi:10.1016/j.micres.2025.128053.

Data availability

Data will be made available on request.

References

Bae, M., Cassilly, C.D., Liu, X., Park, S.M., Tusi, B.K., Chen, X., et al., 2022. Akkermansia muciniphila phospholipid induces homeostatic immune responses. Epub 2022/07/28. Nature 608 (7921), 168–173. https://doi.org/10.1038/s41586-022-04985-7.

Cani, P.D., Depommier, C., Derrien, M., Everard, A., de Vos, W.M., 2022. Akkermansia muciniphila: paradigm for next-generation beneficial microorganisms. Epub 2022/06/01. Nat. Rev. Gastroenterol. Hepatol. 19 (10), 625–637. https://doi.org/10.1038/s41575-022-00631-9.

Cao, J., Qin, L., Zhang, L., Wang, K., Yao, M., Qu, C., et al., 2024. Protective effect of cellulose and soluble dietary fiber from Saccharina japonica by-products on regulating inflammatory responses, gut microbiota, and SCFAs production in colitis mice. Epub 2024/04/06. Int. J. Biol. Macromol. 267 (Pt 1), 131214. https://doi.org/10.1016/j.ijbiomac.2024.131214.

Chao, A., 1984. Non-parametric estimation of the number of classes in a population. Scand. J. Stat. 11, 265–270.

Chen, K.J., Huang, Y.L., Kuo, L.M., Chen, Y.T., Hung, C.F., Hsieh, P.W., 2022. Protective role of casuarinin from Melastoma malabathricum against a mouse model of 5-fluorouracil-induced intestinal mucositis: Impact on inflammation and gut microbiota dysbiosis. Epub 2022/04/18. Phytomedicine: Int. J. Phytother. Phytopharm. 101, 154092. https://doi.org/10.1016/j.phymed.2022.154092.

Chen, Y., Li, Y., Fan, Y., Chen, S., Chen, L., Chen, Y., et al., 2024. Gut microbiota-driven metabolic alterations reveal gut-brain communication in Alzheimer's disease model mice. Epub 2024/01/23. Gut Microbes 16 (1), 2302310. https://doi.org/10.1080/19490976.2024.2302310.

Chen, G., Zhuang, J., Cui, Q., Jiang, S., Tao, W., Chen, W., et al., 2020. Two Bariatric Surgical Procedures Differentially Alter the Intestinal Microbiota in Obesity Patients. Epub 2020/03/11. Obes. Surg. 30 (6), 2345–2361. https://doi.org/10.1007/s11695-020-04494-4.

de la Cuesta-Zuluaga, J., Mueller, N.T., Corrales-Agudelo, V., Velasquez-Mejia, E.P., Carmona, J.A., Abad, J.M., et al., 2017. Metformin Is Associated With Higher Relative Abundance of Mucin-Degrading Akkermansia muciniphila and Several Short-Chain Fatty Acid-Producing Microbiota in the Gut. Epub 2016/12/22. Diabetes Care 40 (1), 54–62. https://doi.org/10.2337/dc16-1324.

Depommier, C., Everard, A., Druart, C., Plovier, H., Van Hul, M., Vieira-Silva, S., et al., 2019. Supplementation with Akkermansia muciniphila in overweight and obese human volunteers: a proof-of-concept exploratory study. Epub 2019/07/03. Nat. Med 25 (7), 1096–1103. https://doi.org/10.1038/s41591-019-0495-2.

Depommier, C., Van Hul, M., Everard, A., Delzenne, N.M., De Vos, W.M., Cani, P.D., 2020. Pasteurized Akkermansia muciniphila increases whole-body energy expenditure and fecal energy excretion in diet-induced obese mice. Epub 2020/03/14. Gut Microbes 11 (5), 1231–1245. https://doi.org/10.1080/19490976.2020.1737307.

Derrien, M., Vaughan, E.E., Plugge, C.M., de Vos, W.M., 2004. Akkermansia muciniphila gen. nov., sp. nov., a human intestinal mucin-degrading bacterium. Epub 2004/09/25. Int J. Syst. Evol. Microbiol 54 (Pt 5), 1469–1476. https://doi.org/10.1099/ijs.0.02873-0.

Duca, F.A., Côté, C.D., Rasmussen, B.A., Zadeh-Tahmasebi, M., Rutter, G.A., Filippi, B. M., et al., 2015. Metformin activates a duodenal Ampk-dependent pathway to lower hepatic glucose production in rats. Epub 2015/04/08. Nat. Med 21 (5), 506–511. https://doi.org/10.1038/nm.3787.

Everard, A., Belzer, C., Geurts, L., Ouwerkerk, J.P., Druart, C., Bindels, L.B., et al., 2013. Cross-talk between Akkermansia muciniphila and intestinal epithelium controls diet-induced obesity. Epub 2013/05/15. Proc. Natl. Acad. Sci. USA 110 (22), 9066–9071. https://doi.org/10.1073/pnas.1219451110.

Gawlik, A.M., Shmoish, M., Hartmann, M.F., Wudy, S.A., Hochberg, Z., 2020. Steroid Metabolomic Signature of Insulin Resistance in Childhood Obesity. Epub 2019/11/16. Diabetes Care 43 (2), 405–410. https://doi.org/10.2337/dc19-1189.

Guo, H., Fu, X., He, J., Wang, R., Yan, M., Wang, J., et al., 2023. Gut bacterial consortium enriched in a biofloc system protects shrimp against Vibrio parahaemolyticus infection. Epub 2023/10/20. Microbiome 11 (1), 230. https://doi.org/10.1186/s40168-023-01663-2.

Hardie, D.G., Ross, F.A., Hawley, S.A., 2012. AMPK: a nutrient and energy sensor that maintains energy homeostasis. Epub 2012/03/23. Nat. Rev. Mol. Cell Biol. 13 (4), 251–262. https://doi.org/10.1038/nrm3311.

Harmel, E., Grenier, E., Bendjoudi Ouadda, A., El Chebly, M., Ziv, E., Beaulieu, J.F., et al., 2014. AMPK in the small intestine in normal and pathophysiological conditions. Epub 2014/01/16. Endocrinology 155 (3), 873–888. https://doi.org/10.1210/en.2013-1750.

Jia, S., Ivanov, A., Blasevic, D., Muller, T., Purfurst, B., Sun, W., et al., 2015. Insm1 cooperates with Neurod1 and Foxa2 to maintain mature pancreatic beta-cell function. Epub 2015/04/02. EMBO J. 34 (10), 1417–1433. https://doi.org/10.15252/embj.201490819.

Karlsson, C.L., Onnerfalt, J., Xu, J., Molin, G., Ahrne, S., Thorngren-Jerneck, K., 2012. The microbiota of the gut in preschool children with normal and excessive body weight. Epub 2012/05/02. Obes. (Silver Spring) 20 (11), 2257–2261. https://doi.org/10.1038/oby.2012.110.

Ko, C.W., Qu, J., Black, D.D., Tso, P., 2020. Regulation of intestinal lipid metabolism: current concepts and relevance to disease. Epub 2020/02/06. Nat. Rev. Gastroenterol. Hepatol. 17 (3), 169–183. https://doi.org/10.1038/s41575-019-0250-7.

Lema, I., Araujo, J.R., Rolhion, N., Demignot, S., 2020. Jejunum: The understudied meeting place of dietary lipids and the microbiota. Epub 2020/09/20. Biochimie 178, 124–136. https://doi.org/10.1016/j.biochi.2020.09.007.

Li, J., Zhao, F., Wang, Y., Chen, J., Tao, J., Tian, G., et al., 2017. Gut microbiota dysbiosis contributes to the development of hypertension. Epub 2017/02/02. Microbiome 5 (1), 14. https://doi.org/10.1186/s40168-016-0222-x.

Liang, X., Duan, H., Mao, Y., Koestner, U., Wei, Y., Deng, F., et al., 2021. The SNAG Domain of Insm1 Regulates Pancreatic Endocrine Cell Differentiation and Represses beta- to delta-Cell Transdifferentiation. Epub 2021/02/07. Diabetes 70 (5), 1084–1097. https://doi.org/10.2337/db20-0883.

Liu, T.H., Wang, J., Zhang, C.Y., Zhao, L., Sheng, Y.Y., Tao, G.S., et al., 2023. Gut microbial characteristical comparison reveals potential anti-aging function of Dubosiella newyorkensis in mice. Epub 2023/02/18. Front. Endocrinol. 14, 1133167. https://doi.org/10.3389/fendo.2023.1133167.

Lkhagva, E., Chung, H.J., Hong, J., Tang, W.H.W., Lee, S.I., Hong, S.T., et al., 2021. The regional diversity of gut microbiome along the GI tract of male C57BL/6 mice. Epub 2021/02/14. BMC Microbiol 21 (1), 44. https://doi.org/10.1186/s12866-021-02099-0.

Ma, H., Xiong, H., Zhu, X., Ji, C., Xue, J., Li, R., et al., 2019. Polysaccharide from Spirulina platensis ameliorates diphenoxylate-induced constipation symptoms in mice. Epub 2019/05/06. Int. J. Biol. Macromol. 133, 1090–1101. https://doi.org/10.1016/j.ijbiomac.2019.04.209.

Nagarajan, A., Lasher, A.T., Morrow, C.D., Sun, L.Y., 2024. Long term methionine restriction: Influence on gut microbiome and metabolic characteristics. Epub 2024/01/27. Aging Cell 23 (3), e14051. https://doi.org/10.1111/acel.14051.

Ochiai, M., 2020. Evaluating the appropriate oral lipid tolerance test model for investigating plasma triglyceride elevation in mice. Epub 2020/10/07. PLoS One 15 (10), e0235875. https://doi.org/10.1371/journal.pone.0235875.

Plovier, H., Everard, A., Druart, C., Depommier, C., Van Hul, M., Geurts, L., et al., 2017. A purified membrane protein from Akkermansia muciniphila or the pasteurized bacterium improves metabolism in obese and diabetic mice. Epub 2016/11/29. Nat. Med 23 (1), 107–113. https://doi.org/10.1038/nm.4236.

Rena, G., Hardie, D.G., Pearson, E.R., 2017. The mechanisms of action of metformin. Epub 2017/08/05. Diabetologia 60 (9), 1577–1585. https://doi.org/10.1007/s00125-017-4342-z.

Santacruz, A., Collado, M.C., Garcia-Valdes, L., Segura, M.T., Martin-Lagos, J.A., Anjos, T., et al., 2010. Gut microbiota composition is associated with body weight, weight gain and biochemical parameters in pregnant women. Epub 2010/03/09. Br. J. Nutr. 104 (1), 83–92. https://doi.org/10.1017/S0007114510000176.

Schnupf, P., Gaboriau-Routhiau, V., Cerf-Bensussan, N., 2013. Host interactions with Segmented Filamentous Bacteria: an unusual trade-off that drives the post-natal

maturation of the gut immune system. Epub 2013/11/05. Semin. Immunol. 25 (5), 342–351. https://doi.org/10.1016/j.smim.2013.09.001.
Schnupf, P., Gaboriau-Routhiau, V., Gros, M., Friedman, R., Moya-Nilges, M., Nigro, G., et al., 2015. Growth and host interaction of mouse segmented filamentous bacteria in vitro. Epub 2015/01/21. Nature 520 (7545), 99–103. https://doi.org/10.1038/nature14027.
Shannon, C.E., 1948. A mathematical theory of communication. Bell Syst. Tech. J. 27, 379–423, 623–56.
Shin, N.R., Lee, J.C., Lee, H.Y., Kim, M.S., Whon, T.W., Lee, M.S., et al., 2014. An increase in the Akkermansia spp. population induced by metformin treatment improves glucose homeostasis in diet-induced obese mice. Epub 2013/06/28. Gut 63 (5), 727–735. https://doi.org/10.1136/gutjnl-2012-303839.
Tao, W., Ye, Z., Wei, Y., Wang, J., Yang, W., Yu, G., et al., 2023. Insm1 regulates mTEC development and immune tolerance. Epub 2023/11/22. Cell Mol. Immunol. 20 (12), 1472–1486. https://doi.org/10.1038/s41423-023-01102-0.
Tao, W., Zhang, Y., Ma, L., Deng, C., Duan, H., Liang, X., et al., 2018. Haploinsufficiency of Insm1 Impairs Postnatal Baseline beta-Cell Mass. Epub 2018/09/28. Diabetes 67 (12), 2615–2625. https://doi.org/10.2337/db17-1330.
Tomas, J., Mulet, C., Saffarian, A., Cavin, J.B., Ducroc, R., Regnault, B., et al., 2016. High-fat diet modifies the PPAR-γ pathway leading to disruption of microbial and physiological ecosystem in murine small intestine. E5934-e43. Epub 2016/09/18. Proc. Natl. Acad. Sci. USA 113 (40). https://doi.org/10.1073/pnas.1612559113.
Tung, Y.C., Liang, Z.R., Yang, M.J., Ho, C.T., Pan, M.H., 2022. Oolong tea extract alleviates weight gain in high-fat diet-induced obese rats by regulating lipid metabolism and modulating gut microbiota. Epub 2022/02/19. Food Funct. 13 (5), 2846–2856. https://doi.org/10.1039/d1fo03356e.
Wang, J., Chen, G., Cui, Q., Song, E., Tao, W., Chen, W., et al., 2019b. Renal Subcapsular Transplantation of 2′-Deoxyguanosine-Treated Murine Embryonic Thymus in Nude Mice. J. Vis. Exp. (149).
Wang, J., Lang, T., Shen, J., Dai, J., Tian, L., Wang, X., 2019a. Core Gut Bacteria Analysis of Healthy Mice. Epub 2019/05/21. Front. Microbiol. 10, 887. https://doi.org/10.3389/fmicb.2019.00887.
Wang, J., Qie, J., Zhu, D., Zhang, X., Zhang, Q., Xu, Y., et al., 2022. The landscape in the gut microbiome of long-lived families reveals new insights on longevity and aging - relevant neural and immune function. Epub 2022/08/09. Gut Microbes 14 (1), 2107288. https://doi.org/10.1080/19490976.2022.2107288.
Yan, G., Li, S., Wen, Y., Luo, Y., Huang, J., Chen, B., et al., 2022. Characteristics of intestinal microbiota in C57BL/6 mice with non-alcoholic fatty liver induced by high-fat diet. Epub 2023/01/10. Front. Microbiol. 13, 1051200. https://doi.org/10.3389/fmicb.2022.1051200.
Ye, X., Sun, P., Lao, S., Wen, M., Zheng, R., Lin, Y., et al., 2023. Fgf21-Dubosiella axis mediates the protective effects of exercise against NAFLD development. Life Sci. 334, 122231.
Yoon, H.S., Cho, C.H., Yun, M.S., Jang, S.J., You, H.J., Kim, J.H., et al., 2021. Akkermansia muciniphila secretes a glucagon-like peptide-1-inducing protein that improves glucose homeostasis and ameliorates metabolic disease in mice. Epub 2021/04/07. Nat. Microbiol 6 (5), 563–573. https://doi.org/10.1038/s41564-021-00880-5.
Zhang, X., Shen, D., Fang, Z., Jie, Z., Qiu, X., Zhang, C., et al., 2013. Human gut microbiota changes reveal the progression of glucose intolerance. Epub 2013/09/10. PLoS One 8 (8), e71108. https://doi.org/10.1371/journal.pone.0071108.
Zhang, Y., Tu, S., Ji, X., Wu, J., Meng, J., Gao, J., et al., 2024. Dubosiella newyorkensis modulates immune tolerance in colitis via the L-lysine-activated AhR-IDO1-Kyn pathway. Epub 2024/02/14. Nat. Commun. 15 (1), 1333. https://doi.org/10.1038/s41467-024-45636-x.